ROYAL SOCIETY
OF CHEMISTRY

COMMUNICATION

Check for updates

How carbon contamination on the photocatalysts interferes with the performance analysis of CO$_2$ reduction†

Jiakang You,[a] Mu Xiao,[a] Siqi Liu, [iD][a] Haijiao Lu,[a] Peng Chen, [iD][a] Zhi Jiang, [iD][b] Wenfeng Shangguan,[b] Zhiliang Wang [iD]*[a] and Lianzhou Wang [iD]*[a]

Photocatalytic carbon dioxide (CO$_2$) reduction reaction (CO$_2$RR) for the production of valuable chemicals is a promising solar-driven strategy to mitigate CO$_2$ emissions. However, carbon contamination on the photocatalysts interferes with the investigation of CO$_2$RR performance. This work quantitatively investigates the significant impact of carbon contamination on performance analysis of photocatalytic CO$_2$RR, which can lead to false-positive results of photocatalysts with different types of band structure (*i.e.*, TiO$_2$, CuO, and BiVO$_4$) due to photoinduced oxidation process. Moreover, the commonly used organic solvent in a laboratory environment (*e.g.*, ethanol) was proved to have a profound impact on photocatalytic CO$_2$RR behaviour wherein 1 microliter of ethanol could boost the apparent methane generation by 17 times. To solve this issue, oxygen plasma treatment is demonstrated to be effective in removing surface carbon contamination. To minimise the impact of surface carbon contamination and eliminate false-positive results, it is expected to further enhance the photocatalytic performance and store catalysts in a carbon-free atmosphere.

The rapid consumption of fossil fuels in human activities, such as transport, industry, and household sectors, causes a striking increase in CO$_2$ concentration in the atmosphere, leading to serious environmental issues, such as global warming and ocean acidification.[1,2] Thus, these problems must urgently be addressed by reducing CO$_2$ emissions and making full utilisation of the existing CO$_2$. Photocatalytic CO$_2$ reduction reaction (CO$_2$RR) has attracted global research interest over the past decades.[3] In an ideal process, it is expected that the photogenerated electrons in the photocatalysts are applied to reduce

CO$_2$, meanwhile, photogenerated holes are consumed for water oxidation. Considering the stable structure of CO$_2$ with a high bond energy of 750 kJ mol^{-1},[4] there is a high energy barrier for the activation of CO$_2$, which requires sophisticated photocatalyst designs.

Despite tremendous research efforts, the production rates of carbon monoxide (CO) and methane (CH$_4$), which are the most common products, stay at low levels (*e.g.*, <17.33 μmol g^{-1} h^{-1} for CO and <2000 μmol g^{-1} h^{-1} for CH$_4$).[5–12] However, external factors, such as organic vapours in a lab, surface carbon contamination, *etc.*, are more likely to produce these carbon products *via* oxidation reaction, other than CO$_2$ reduction, and therefore they might result in false-positive signals. For example, methanol (CH$_3$OH), a common hole scavenger in photocatalytic reactions, can produce significant amounts of CO through a photocatalytic oxidation process.[13–16] Although isotope analysis is regarded as an effective approach to verify the carbon source by tracing the ^{13}C transfer from CO$_2$ molecules to the products, the possible isotopic substitution makes this method less reliable.[17–20] To provide reproducible and convincing data for CO$_2$RR analysis, some recent perspectives invoked the elimination of contamination sources as completely as possible.[21,22] Yet, there is still no quantitative investigation on how carbon contamination interferes with the performance analysis of photocatalytic CO$_2$RR.

In this work, we have provided a quantitative analysis of the apparently over-estimated product amount due to hole-induced contamination oxidation, other than the CO$_2$RR process. Photocatalysts with different valence band (VB) positions have been applied to verify that the contamination oxidation reaction exaggerates the apparent CO$_2$RR activity. Using a prototypical Au/TiO$_2$ photocatalyst for CO$_2$RR, introducing a trace amount (*i.e.*, 1 μL) of ethanol (EtOH) caused over 17 times higher CH$_4$ production rate and higher stability for CO production. Moreover, facile oxygen plasma pre-treatment was confirmed to be an effective protocol to minimise the influence of carbon contamination during gas-phase photocatalytic CO$_2$ conversion. These findings provide new insights into CO$_2$RR research

[a]*Nanomaterials Centre, School of Chemical Engineering and Australian Institute for Bioengineering and Nanotechnology, The University of Queensland, St Lucia, Queensland, 4072, Australia*

[b]*Research Center for Combustion and Environment Technology, Shanghai Jiao Tong University, Shanghai, 200240, China. E-mail: zhiliang.wang@uq.edu.au; l.wang@uq.edu.au*

and will enable the acquisition of more consistent and reliable quantitative results across the research community.

The Au/TiO_2 has been intensively investigated to be an effective photocatalyst for CO_2RR, which makes it a good benchmark for investigating the carbon contamination issue. The prototypical Au/TiO_2 photocatalysts have been widely reported to be active towards gas-phase CO_2 conversion to CO and CH_4, with a production rate ranging from 3 to 210 $\mu mol\ g^{-1}\ h^{-1}$ depending on reaction conditions.[5,23] Considering the ultralow dosage of photocatalyst (*c.a.* 10 mg) in the reported research, the absolute yields of CO_2RR products are negligible. In our research, we adopted a similar procedure to coat the as-prepared Au/TiO_2 photocatalyst (ESI†) on a glass substrate with a rough surface. Herein, Au was deposited *via* chemical reduction by sodium borohydride to avoid introducing organic sources on the TiO_2 surface.[24–26] The X-ray diffraction (XRD) (Fig. S1†) and transmission electronic microscopy (TEM) (Fig. S2†) of the as-produced Au/TiO_2 indicate that the Au nanoparticles were deposited on the TiO_2 surface.

Photocatalytic CO_2 conversion was carried out in a batch reactor, wherein the system was filled with pure CO_2 (>99.9%) before turning on the lighting (ESI†). Fig. 1a and b show the CO and CH_4 with a mass-specific production (MSP) of 30 $\mu mol\ g^{-1}$ and 67.5 $\mu mol\ g^{-1}$, respectively, in 90 minutes. This photocatalytic activity is comparable to literature results based on similar Au/TiO_2 systems.[27–31] Unexpectedly, in the controlled experiment, where the photocatalytic system was filled with argon gas (Ar), obvious CH_4 and CO production was also detected. Especially, the absolute yields of CH_4 were very close to the case in the presence of CO_2, indicating that the apparent CO_2RR activity has been overestimated as shown in Fig. 1b. In addition, profound H_2 production (Fig. S3†) was observed in both cases (while no oxygen was detected), which may lead to a noticeable CO decrease as shown in Fig. 1a *via* hydrogenation. With the above results, there is a question on the origin of CO and CH_4 under an Ar atmosphere.

X-ray photoelectron spectroscopy (XPS) was used to determine the surface chemical environment of TiO_2 (Fig. 1c). Although we avoided the organic sources during photocatalyst preparation, the carbon peak could always be observed even on the pure inorganic metallic samples, which is indexed to ubiquitous carbon contamination from air exposure.[32] This peak is commonly used as a reference value to calibrate XPS

data, representing C–C or C–H bond.[32–34] These carbon species can produce extra CO or CH_4 with the interaction with the photogenerated charges.

The applied TiO_2 holds a large bandgap, where it is capable of producing CO and CH_4 either by CO_2 reduction reaction or *via* carbon contamination oxidation. To get more insight into whether photogenerated electrons or holes contribute more to the CO and CH_4 generation, the other two semiconductors, $BiVO_4$ and CuO, were selected due to their band structure features (Fig. 2a, see ESI† for details on preparation). Ultraviolet photoelectron spectroscopy (UPS) and ultraviolet-visible (UV-vis) spectroscopy were used to further determine the band positions as shown in Fig. S4 and S5.† The properties of the valence band (VB) and conduction band (CB) of BVO_4, CuO, and TiO_2 are summarised in Fig. 2a, which shows the CB of CuO and VB of $BiVO_4$ to be close to the CB and VB of TiO_2, respectively, in accordance with the literature.[35–37] From the relative position of CB (−3.73 eV) to the redox potential of CO_2/CO (−4.38 eV) and CO_2/CH_4 (−4.67 eV), it can be concluded that only CuO can facilitate the CO_2RR. While the relatively shallow VB (−5.05 eV) of CuO makes it unlikely to process contamination oxidation. The $BiVO_4$ has the opposite situation in that CO_2RR is unlikely to happen due to the thermodynamic limit of CB (−5.03 eV), but the contamination oxidation process is relatively easy due to the deep VB (−7.43 eV). Therefore, the photocatalytic performance of CuO and $BiVO_4$ can help distinguish whether the CO_2RR or oxidation of carbon contaminations contributes to the apparent CO and CH_4 generation. Surface carbon content on the TiO_2, CuO, and $BiVO_4$ was determined to be 14.96, 26.02, and 8.44 wt%, respectively, as analysed by XPS (Table S1†).

Their photocatalytic performance is shown in Fig. 2b and c and S7.† Interestingly, $BiVO_4$ produced significant amounts of CH_4 (5.4 $\mu mol\ g^{-1}$) and CO (13.5 $\mu mol\ g^{-1}$), while CuO produced nearly null. As mentioned above, products from $BiVO_4$ indicate that carbon contamination oxidation occurs, which can lead to false-positive CO_2RR results, despite the consensus that $BiVO_4$ is not capable of this process. Another photocatalyst, SnO_2, also possesses a low CB which is challenged for CO_2RR.[38] However, a considerable amount of CH_4 (3.8 $\mu mol\ g^{-1}$) and CO (13.1 $\mu mol\ g^{-1}$) is observed upon light irradiation (Fig. S8†). We suppose this is also a false-positive result for CO_2RR caused by carbon contamination oxidation. The absence of a product from CuO
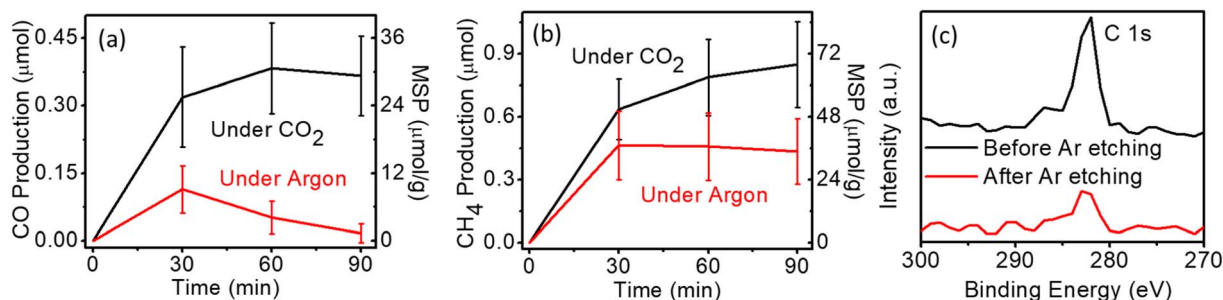

Fig. 1 (a) CO production and (b) CH_4 production from photocatalytic reactions on Au/TiO_2 in CO_2 (black line) or Ar (red line). (c) Comparison of C 1s XPS spectrum of the same TiO_2 sample before and after Ar etching. MSP: mass-specific production.
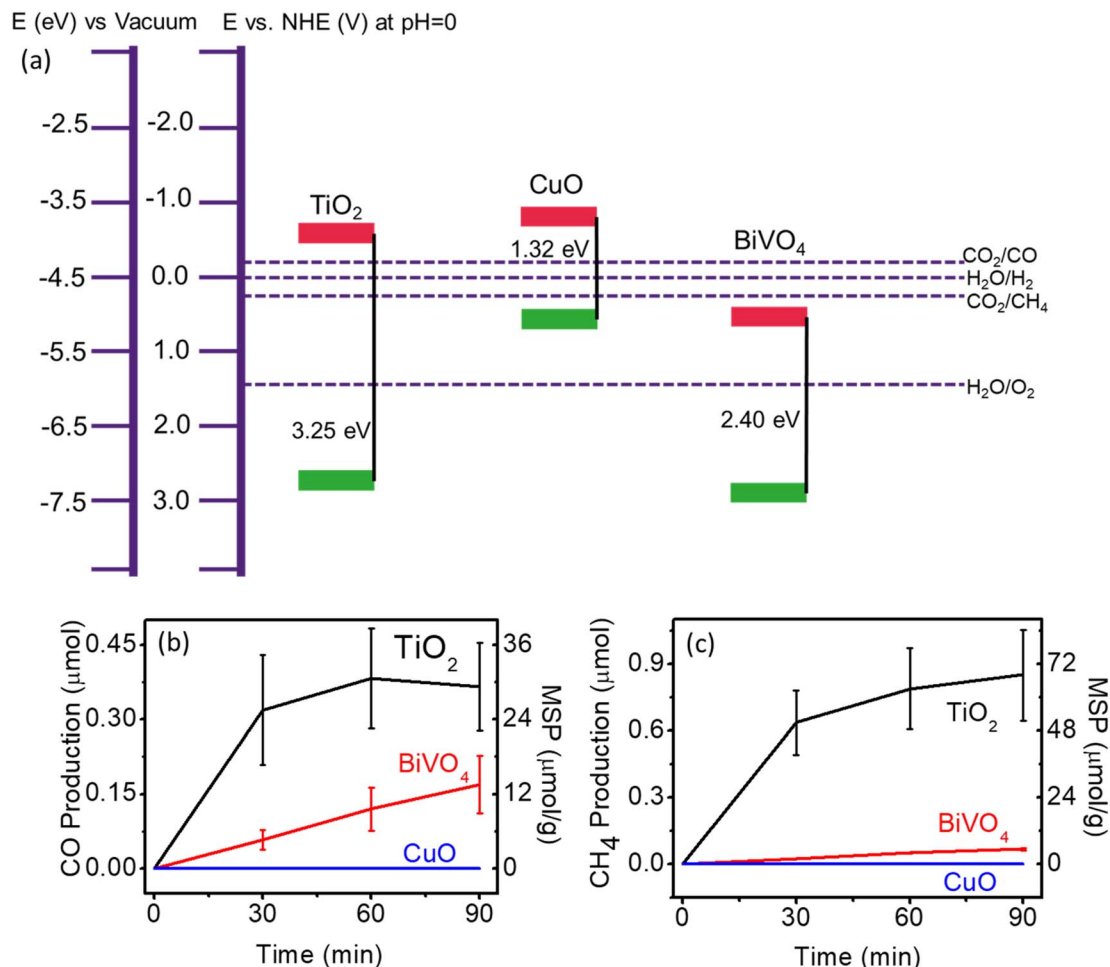
10150 | *J. Mater. Chem. A*, 2023, **11**, 10149–10154

This journal is © The Royal Society of Chemistry 2023

Fig. 2 (a) Band position of TiO_2, CuO, and $BiVO_4$ in line with CO_2RR, redox potentials of hydrogen and oxygen evolution reactions. Photocatalytic CO_2RR performance over TiO_2, CuO, and $BiVO_4$ (b) CO production; (c) CH_4 production. MSP: mass-specific production.

further indicates the significance of the oxidation process for the apparent CO and CH_4 generation.

Carbon-containing photocatalysts have been extensively researched for CO_2RR because of their attractive physicochemical properties. Graphitic carbon nitride (g-C_3N_4) is one of the most investigated metal-free organic photocatalysts due to its low cost, visible light harvesting, and suitable band position

for CO_2RR.[39] However, the carbon in g-C_3N_4 will interfere with the CO_2RR performance analysis. Fig. 3 shows the photocatalytic performance on g-C_3N_4 under Ar and CO_2 atmospheres. The production rates of CO (47.1 μmol g^{-1}) and CH_4 (3.5 μmol g^{-1}) under the Ar atmosphere have very small and even negligible difference, as compared to the rates under the CO_2 atmosphere. These results are consistent with the report of
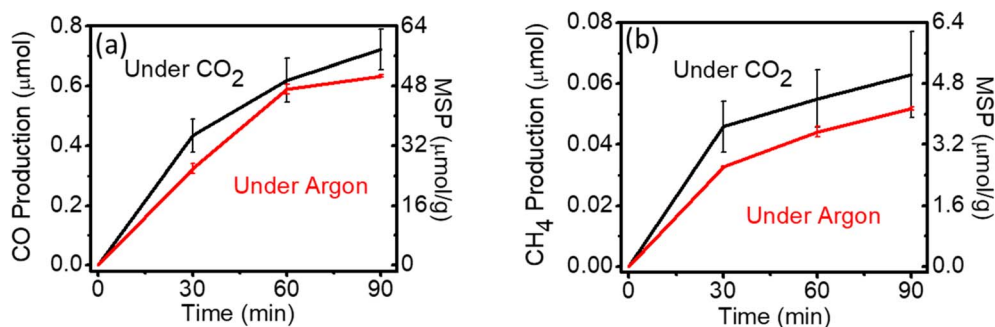

Fig. 3 (a) CO production and (b) CH_4 production from photocatalytic reactions on g-C_3N_4 in CO_2 (black line) or Ar (red line). MSP: mass-specific production.

light-induced self-decomposition of g-C_3N_4, rather than CO_2RR.[40] Theoretical calculations have indicated that self-decomposition reaction is thermodynamically more favourable than CO_2RR.[40]

The impact of organic pollution on photocatalytic CO_2RR is even more pronounced in the presence of ethanol (EtOH), which is a widely used organic solvent for synthesis and a sacrificial agent for photocatalysis. Take the Au/TiO_2 system as an example, when 1 μL of EtOH is deliberately added to the reaction system, the CH_4 production rate was boosted by 17 times from 68 μmol g^{-1} to 1244.8 μmol g^{-1} as shown in Fig. 4a because of the alcohol and carboxyl acid decomposition under the light.[41–45] Meanwhile, a large amount of hydrogen was produced (Fig. S7†), which could inhibit the generation of CO as shown in Fig. 4b. The photocatalytic performance of pure TiO_2 was also evaluated as a reference (Fig. S9†), which showed overall lower activity in the absence of Au cocatalyst. A plausible pathway for EtOH oxidation under light is shown in Fig. 4c. Upon light irradiation, ethanol was oxidised to ethanal with hydrogen generation. Ethanal can be decomposed via three different routes to mislead the photocatalytic CO_2RR test. Ethanal can be directly converted to CO_2 and hydrogen via the photocatalytic process. Under ambient conditions, some of the ethanal decomposes to produce CH_4 and CO spontaneously.

While, in some cases, the above products would be further oxidised to acetic acid and H_2 with acetic acid being further decomposed to CH_4 and CO_2 upon light illumination. Thus, the introduction of EtOH into the reaction system not only affects the activity analysis, but also influences the selectivity analysis (Table S2†) with considerable hydrogen production (Fig. S7†). Therefore, possible false-positive results can be obtained due to the organic residuals in the system, which must be eliminated when conducting photocatalytic CO_2RR experiments. Due to the dramatic performance boost by the trace amount of EtOH, researchers in this field should be extremely careful about organic solvent vapours generated in the laboratory environment.

Oxygen plasma treatment is commonly used to eliminate residual organic ligands from the material surface. To avoid the interference of surface contamination, oxygen plasma cleaning was performed to etch the surface of the photocatalyst (i.e., Au/TiO_2). Fig. 5 and S10† show the photocatalytic performance of treated Au/TiO_2 photocatalysts. In the Ar environment, the CO and CH_4 production rates decreased dramatically to a negligible level, especially for CH_4; the production rate for CH_4 dropped from 34 to 4.69 μmol g^{-1}, indicating the effectiveness of the oxygen plasma treatment. Therefore, oxygen plasma treatment can be used to effectively clean the surface of the materials
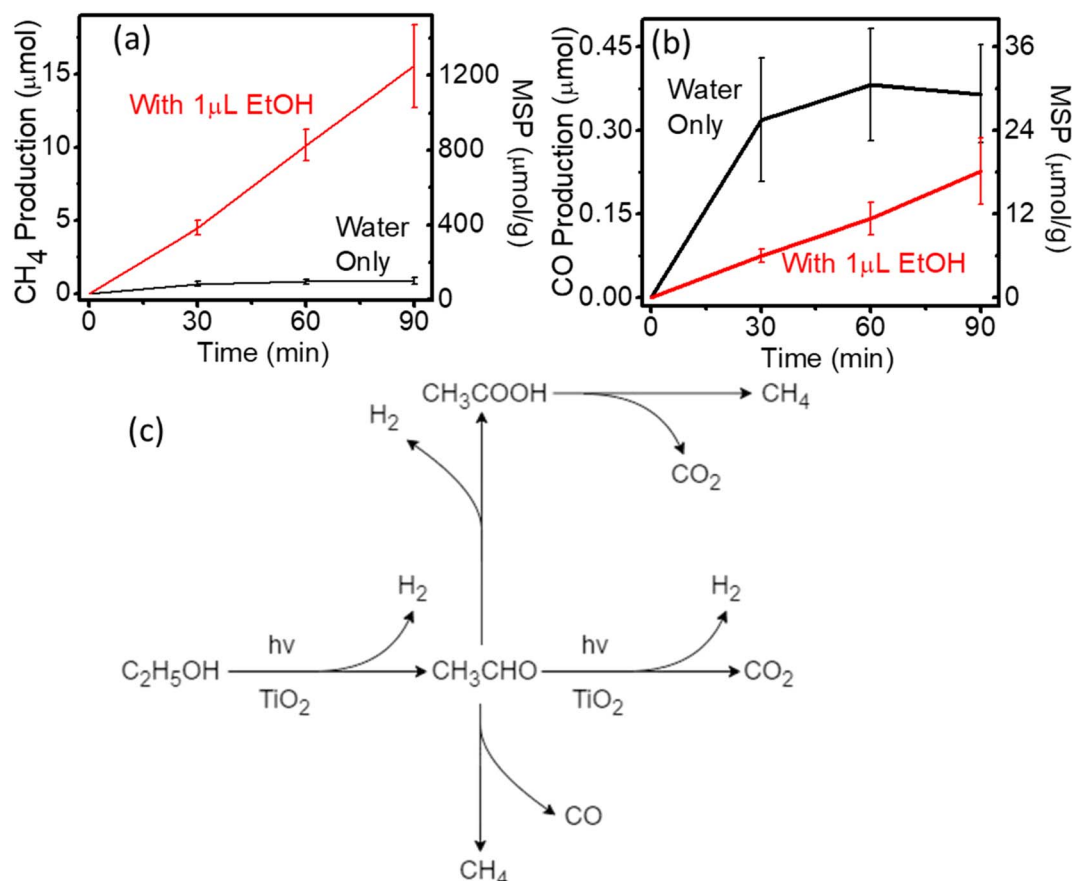

Fig. 4 Photocatalytic performance of Au/TiO_2 with different solvents (a) CO production; (b) CH_4 production. (c) Schematic illustration of photocatalytic ethanol oxidation. MSP: mass-specific production.
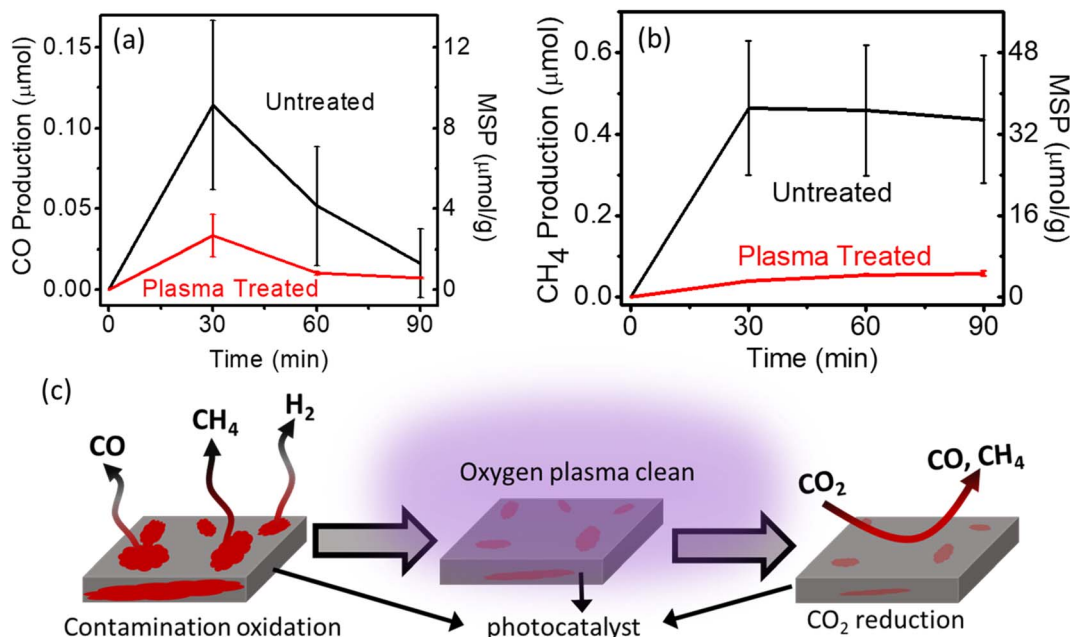
10152 | J. Mater. Chem. A, 2023, **11**, 10149–10154

This journal is © The Royal Society of Chemistry 2023

Fig. 5 Controlled experiments before and after plasma treatment under the Ar atmosphere (a) CO production; (b) CH_4 production. MSP: mass-specific production rate. (c) schematic representation of oxygen plasma cleaning.

before conducting photocatalytic experiments as shown in Fig. 5c.

In summary, we have quantitatively shown the influence of carbon contamination on photocatalysts during photocatalytic CO_2RR activities. When the photocatalytic CO_2RR activity is low, the impact of the carbon contamination oxidation is therefore significant. The commonly used organic solvent in laboratories (e.g., ethanol) was demonstrated to have a serious impact on photocatalytic CO_2RR behaviour, leading to false-positive results. To address this issue, oxygen plasma treatment is effective in removing carbon contamination by cleaning the surface of the materials before conducting photocatalytic experiments. The reason for such a significant impact of carbon contamination is the extremely low production rate and carbon conversion rates of photocatalytic CO_2RR.[46–49] If the production and carbon conversion rates are high enough (e.g., >10 mmol g^{-1} h^{-1}), the carbon contamination issue would be negligible. Some strategies can be utilised for higher CO_2RR performance, such as defect engineering, nanostructure design, cocatalysts design, heterostructure design, and Z-scheme construction. Furthermore, photocatalysts should be stored in a carbon-free environment (e.g., an N_2/Ar-filled glove box), if possible, to minimise carbon contamination. Long-term stability tests could decrease the effect of carbon contaminations. Future research should focus on improving the production rate and selectivity and developing highly efficient photocatalysts for CO_2RR.

Conflicts of interest

There are no conflicts to declare.

Acknowledgements

References

1 Global Monitoring Laboratory, Trends in Atmospheric Carbon Dioxide, https://gml.noaa.gov/ccgg/trends/mlo.html, accessed November 1, 2021.

2 R. Heinberg, in The Community Resilience Reader: Essential Resources for an Era of Upheaval, ed. D. Lerch, Island Press/Center for Resource Economics, Washington, DC, 2017, pp. 65–78, DOI: 10.5822/978-1-61091-861-9_4.

3 T. Inoue, A. Fujishima, S. Konishi and K. Honda, Nature, 1979, 277, 637–638.

4 X. Chang, T. Wang and J. Gong, Energy Environ. Sci., 2016, 9, 2177–2196.

5 Ș. Neațu, J. A. Maciá-Agulló, P. Concepción and H. Garcia, J. Am. Chem. Soc., 2014, 136, 15969–15976.

6 V. A. de la Peña O'Shea, D. P. Serrano and J. M. Coronado, in *From Molecules to Materials: Pathways to Artificial Photosynthesis*, ed. E. A. Rozhkova and K. Ariga, Springer International Publishing, Cham, 2015, DOI: 10.1007/978-3-319-13800-8_7, pp. 171–191.

7 H. Shen, T. Peppel, J. Strunk and Z. Sun, *Sol. RRL*, 2020, **4**, 1900546.

8 U. Ulmer, T. Dingle, P. N. Duchesne, R. H. Morris, A. Tavasoli, T. Wood and G. A. Ozin, *Nat. Commun.*, 2019, **10**, 3169.

9 Z. Jiang, H. Sun, T. Wang, B. Wang, W. Wei, H. Li, S. Yuan, T. An, H. Zhao, J. Yu and P. K. Wong, *Energy Environ. Sci.*, 2018, **11**, 2382–2389.

10 W. Shangguan, Q. Liu, Y. Wang, N. Sun, Y. Liu, R. Zhao, Y. Li, C. Wang and J. Zhao, *Nat. Commun.*, 2022, **13**, 3894.

11 W. Wang, C. Deng, S. Xie, Y. Li, W. Zhang, H. Sheng, C. Chen and J. Zhao, *J. Am. Chem. Soc.*, 2021, **143**, 2984–2993.

12 F. Chen, Z. Ma, L. Ye, T. Ma, T. Zhang, Y. Zhang and H. Huang, *Adv. Mater.*, 2020, **32**, 1908350.

13 M. Xiao, L. Zhang, B. Luo, M. Lyu, Z. Wang, H. Huang, S. Wang, A. Du and L. Wang, *Angew. Chem., Int. Ed.*, 2020, **59**, 7230–7234.

14 J. Zhao, R. Shi, Z. Li, C. Zhou and T. Zhang, *Nano Select*, 2020, **1**, 12–29.

15 M. Whitbeck, *Atmos. Environ.*, 1983, **17**, 121–126.

16 A. Kudo and Y. Miseki, *Chem. Soc. Rev.*, 2009, **38**, 253–278.

17 N. N. Lavrentieva, A. S. Dudaryonok and J. V. Buldyreva, *Atmos. Oceanic Opt.*, 2012, **25**, 311–316.

18 O. A. Schaeffer and H. R. Owen, *J. Chem. Phys.*, 1955, **23**, 1305–1309.

19 K. Zhang, Q. Gao, C. Xu, D. Zhao, Q. Zhu, Z. Zhu, J. Wang, C. Liu, H. Yu, C. Sun, X. Liu and Y. Xuan, *Carbon Neutrality*, 2022, **1**, 10.

20 M. Heuillet, F. Bellvert, E. Cahoreau, F. Letisse, P. Millard and J.-C. Portais, *Anal. Chem.*, 2018, **90**, 1852–1860.

21 Y. Zhang, D. Yao, B. Xia, M. Jaroniec, J. Ran and S.-Z. Qiao, *ACS Energy Lett.*, 2022, 1611–1617, DOI: 10.1021/acsenergylett.2c00427.

22 R. Das, S. Chakraborty and S. C. Peter, *ACS Energy Lett.*, 2021, **6**, 3270–3274.

23 H. Zhao, X. Zheng, X. Feng and Y. Li, *J. Phys. Chem. C*, 2018, **122**, 18949–18956.

24 M. V. Dozzi, L. Prati, P. Canton and E. Selli, *Phys. Chem. Chem. Phys.*, 2009, **11**, 7171–7180.

25 C. Deraedt, L. Salmon, S. Gatard, R. Ciganda, R. Hernandez, J. Ruiz and D. Astruc, *Chem. Commun.*, 2014, **50**, 14194–14196.

26 J. Polte, R. Erler, A. F. Thünemann, S. Sokolov, T. T. Ahner, K. Rademann, F. Emmerling and R. Kraehnert, *ACS Nano*, 2010, **4**, 1076–1082.

27 N. Shehzad, M. Tahir, K. Johari, T. Murugesan and M. Hussain, *J. CO2 Util.*, 2018, **26**, 98–122.

28 L. Collado, A. Reynal, J. M. Coronado, D. P. Serrano, J. R. Durrant and V. A. de la Peña O'Shea, *Appl. Catal., B*, 2015, **178**, 177–185.

29 W. Hou, W. H. Hung, P. Pavaskar, A. Goeppert, M. Aykol and S. B. Cronin, *ACS Catal.*, 2011, **1**, 929–936.

30 W. Tu, Y. Zhou, H. Li, P. Li and Z. Zou, *Nanoscale*, 2015, **7**, 14232–14236.

31 M. Compagnoni, G. Ramis, F. S. Freyria, M. Armandi, B. Bonelli and I. Rossetti, *Rend. Lincei Sci. Fis. Nat.*, 2017, **28**, 151–158.

32 G. Greczynski and L. Hultman, *ChemPhysChem*, 2017, **18**, 1507–1512.

33 G. Greczynski and L. Hultman, *Sci. Rep.*, 2021, **11**, 11195.

34 Y. Yamada, J. Kim, S. Matsuo and S. Sato, *Carbon*, 2014, **70**, 59–74.

35 R. Marschall, *Adv. Funct. Mater.*, 2014, **24**, 2421–2440.

36 S. J. A. Moniz and J. Tang, *ChemCatChem*, 2015, **7**, 1659–1667.

37 K. Ding, B. Chen, Y. Li, Y. Zhang and Z. Chen, *J. Mater. Chem. A*, 2014, **2**, 8294–8303.

38 J. A. Torres, G. T. S. T. Da Silva, F. Barbosa de Freitas Silva and C. Ribeiro, *ChemPhysChem*, 2020, **21**, 2392–2396.

39 Y. Li, B. Li, D. Zhang, L. Cheng and Q. Xiang, *ACS Nano*, 2020, **14**, 10552–10561.

40 P. Chen, X. a. Dong, M. Huang, K. Li, L. Xiao, J. Sheng, S. Chen, Y. Zhou and F. Dong, *ACS Catal.*, 2022, **12**, 4560–4570.

41 M. A. Nadeem, M. Murdoch, G. I. N. Waterhouse, J. B. Metson, M. A. Keane, J. Llorca and H. Idriss, *J. Photochem. Photobiol., A*, 2010, **216**, 250–255.

42 T. Sakata and T. Kawai, *Chem. Phys. Lett.*, 1981, **80**, 341–344.

43 X. Fu, D. Y. C. Leung, X. Wang, W. Xue and X. Fu, *Int. J. Hydrog. Energy*, 2011, **36**, 1524–1530.

44 S. Jia, X. Shu, H. Song, Z. An, X. Xiang, J. Zhang, Y. Zhu and J. He, *Ind. Eng. Chem. Res.*, 2021, **60**, 12282–12291.

45 C. A. Walenta, S. L. Kollmannsberger, J. Kiermaier, A. Winbauer, M. Tschurl and U. Heiz, *Phys. Chem. Chem. Phys.*, 2015, **17**, 22809–22814.

46 M. Marx, A. Mele, A. Spannenberg, C. Steinlechner, H. Junge, P. Schollhammer and M. Beller, *ChemCatChem*, 2020, **12**, 1603–1608.

47 M. Qureshi and K. Takanabe, *Chem. Mater.*, 2017, **29**, 158–167.

48 K. Takanabe, *J. Catal.*, 2019, **370**, 480–484.

49 C.-H. Lim, S. Ilic, A. Alherz, B. T. Worrell, S. S. Bacon, J. T. Hynes, K. D. Glusac and C. B. Musgrave, *J. Am. Chem. Soc.*, 2019, **141**, 272–280.